New Horizons in Earth Reinforcement – Otani, Miyata & Mukunoki (eds)
© 2008 Taylor & Francis Group, London, ISBN 978-0-415-45775-0

Bearing capacity of reinforced foundation subjected to pull-out loading: 3D model tests and numerical simulation

T. Nakai, F. Zhang, M. Hinokio, H.M. Shahin, M. Kikumoto & S. Yonaha
Nagoya Institute of Technology, Nagoya, Japan

A. Nishio
Mitsubishi Heavy Industry, Mihara, Japan

ABSTRACT: The pile foundation with reinforced bars is put into practical use for increasing uplift bearing capacity of transmission towers and others For investigating the mechanism of such type of reinforced foundation under various loading conditions in real 3D conditions, 3D model tests and the corresponding numerical analyses were performed, in which the insertion direction of reinforcements and the position of reinforcement are different. The test results show that the reinforcements protruded diagonally downward is the most effective under vertically uplift loading in the same way as those in 2D condition. On the other hand, when the direction of the uplift load is inclined, the reinforcing effect decreases with increasing inclined angle. The numerical results in which mechanical behavior of the soil and the reinforcement and frictional behavior between the soil and the reinforcement are taken into account properly describe well the experimental results.

1 INTRODUCTION

Foundations with reinforcements protruded diagonally downward or horizontally from the side of the foundation were developed and put into practice to increase the uplift bearing capacity of electric transmission tower and others (Matsuo and Ueno, 1989; Tokyo Electric Power Company and Dai Nippon Construction, 1990). 2D numerical simulation and model tests have been carried out to investigate the mechanism of reinforcement (Nakai et al., 2001; Hinokio et al., 2007). The numerical and experimental results show that the reinforcements protruded diagonally downward from the side of the foundation are the most effective, when the foundation is uplifted vertically. However, the reinforcements set up at the side of the foundation are not effective against inclined uplift loading.

In the present study, 3D model tests of the foundation with the flexible reinforcements, which have only tensile stiffness, have been carried out under not only vertical uplift loading but also inclined uplift loading to investigate the reinforced mechanism and to develop the most effective foundation under various kinds of loading conditions. We pay attention particularly to the direction of the reinforcements and the position of the reinforcements. In the finite element analyses, subloading t_{ij} model (Nakai & Hinokio 2004) is used as an elastoplastic constitutive model. This model can describe typical stress deformation and strength characteristics of soils such as the influence of intermediate principal stress, the influence of stress path dependency of plastic flow and the influence of density and/or confining pressure.

In addition to the comparison between tests results and computed results in 3D conditions, these results are compared with those in 2D conditions described in another paper (Hinokio et al, 2007).

2 DESCRIPTION OF MODEL TEST AND ANALYSIS

Figure 1 shows the schematic diagram of the model test apparatus. The size of the model ground is 100 cm in width, 80 cm in length and 50 cm in height. Alumina balls, having diameters of 2.0 mm and 3.0 mm and mixed with the ratio of 1:1 in weight, are used as the model ground (unit weight of the mass is 21.5 kN/m^3). The foundation with the length of 23 cm and 6 cm in diameter is set up in model ground where the penetration depth of the foundation is 18 cm. The arrangement patterns of the reinforcements are illustrated in Figure 2. In the case that the reinforcements are set up at the depth of 15 cm of the side of foundation, the length of the reinforcements (5 cm) should be less than the diameter of the foundation (6 cm). This is due to the construction condition – in the actual case, the reinforcements are protruded from the inside of the foundation after construction of the caisson type foundation. Three kinds of the protruded directions

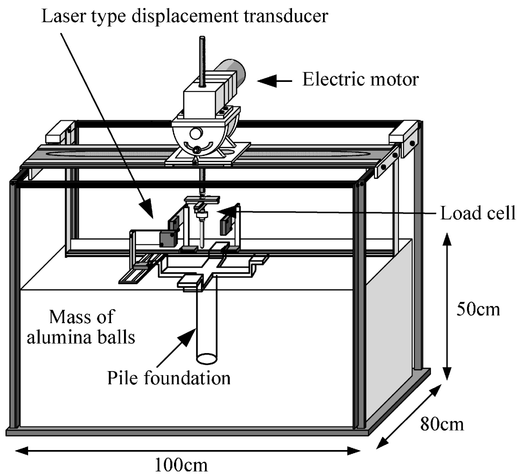

Figure 1. Schematic diagram of the model tests apparatus.

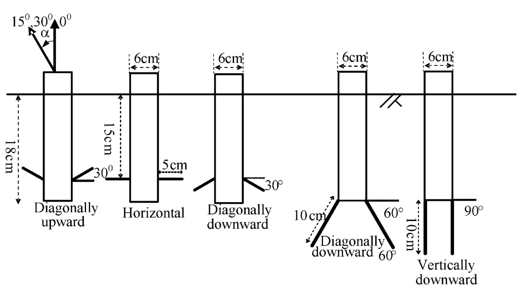

Figure 2. Arrangement of reinforcements.

of reinforcements (diagonally upward, horizontal and diagonallydownward) are employed. In addition to these cases, model tests in which the reinforcements are set up vertically and diagonally downward at the bottom of the foundation are carried out. For these cases, longer reinforcement (10 cm) is protruded from the inside of the foundation.

Aluminum plates with the thickness 0.1 mm and the width of 1 cm are used as the reinforcements for every case. Reinforcement with the thickness of 0.1 mm has enough stiffness against tension but has no bending stiffness. Aluminum plates on which aluminum rods of 1.6 mm in diameter are glued at an equal spacing of 1 cm are used. The friction angle between the reinforcement and the model ground is about 14.5°. Vertical and inclined (angle α is 0°, 15° and 30°) upward displacements are imposed continuously to the foundation. The direction of the uplift load and the plan view of the arrangement of the reinforcements are illustrated in Fig. 3. The uplift load of the foundation is measured by the load cell, and the displacements and rotations of the foundation in three-dimensional space can be grasped by six laser type displace transducers which is arranged around the foundation as shown in Fig. 4. Axial force and bending moment of the reinforcements are measured by the strain gauges that are glued at both sides of the reinforcements.

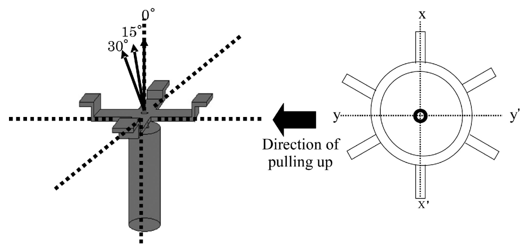

Figure 3. Direction of uplift load and plan view of the arrangement of reinforcements.

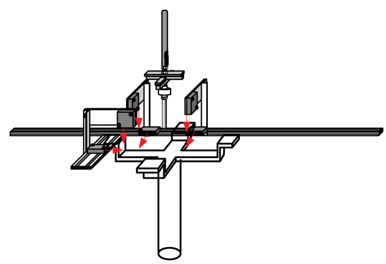

Figure 4. Arrangement of laser type displacement transducer.

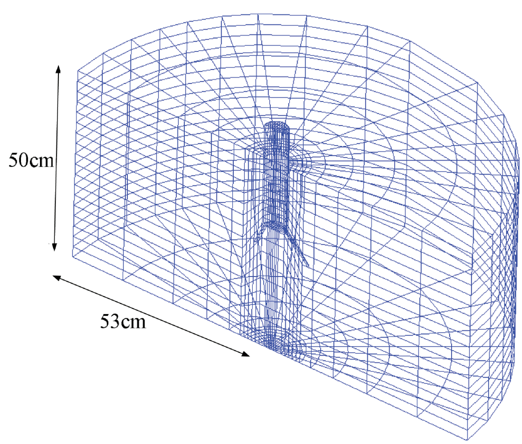

Figure 5. Finite element mesh with diagonally downward reinforcements.

3D finite element analyses under drained condition are carried out in the same scale as the model tests. Finite element meshes for the cases that the reinforcements are protruded diagonally downward from the bottom is shown in Fig. 5. Elastoplastic constitutive model for soils named subloading t_{ij} model (Nakai and

Table 1. Parameters of mass of alumina balls.

Parameters	Value
λ	0.024
κ	0.014
N (e_{NC} *at* $p = 98\,kPa$ & $q = 0\,kPa$)	0.78
$R_{CS} = (\sigma_1/\sigma_3)_{CS(comp.)}$	2.0
β	2.0
ν_e	0.2
a	150

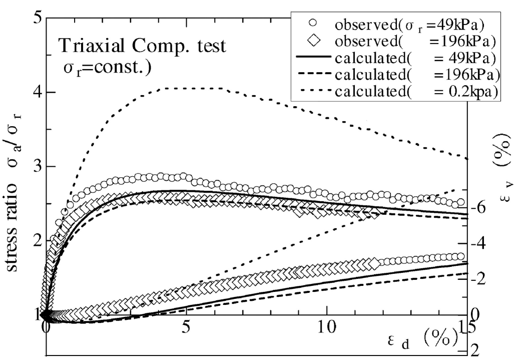

Figure 6. Relationships of stress-strain of alumina balls mass.

Hinokio, 2004) is used. This model can describe properly the following typical characteristics of soils, in spite of its small numbers of parameters: (1) Influence of intermediate principal stress on the deformation and strength of soils. (2) Influence of stress path on the direction of plastic flow, and (3) Influence of density and/or confining pressure. The values of soil parameters for the alumina balls mass are listed in Table 1. Where, λ and κ are the slope of loading and unloading curve of *e-lnp* graphs at the loosest state. N is the void ratio at mean principal stresses (p) 98 kPa in the above mentioned loading curve. β is the model parameter, ν_e is the Poisson's ratio and 'a' represents the influence of density and/or confining pressure. The dots and the solid curves in Fig. 6 are the calculated results corresponding to the observed stress-strain relations (dots) in the triaxial compression tests of the mass of alumina balls, and the dotted curves are the calculated results in which the initial confining pressure is assumed to be two orders smaller in magnitude. This is because the initial confining pressure in model tests is much smaller than that in the triaxial tests. The initial state of the model ground is created by simulating the one-dimensional self-consolidation. The foundation is assumed to be an elastic material with enough stiffness. The reinforcements are simulated by shell elements. Axial stiffness and bending stiffness of each reinforcement is EA = 7.03 × 10 kN and

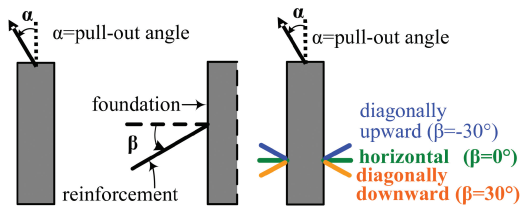

Figure 7. Description of the factors α and β.

$EI = 5.86 \times 10^{-8}$ kN-m^2. In order to model the frictional behavior between the foundation and the ground and between the reinforcements and the ground, an elastoplastic joint element is inserted between them (Nakai, 1985). The friction angle used in the analysis between the foundation and the ground is 8°, and those between the reinforcements and the ground is14.5°.

3 RESULTS AND DISCUSSIONS

3.1 *Reinforcements protruded from the side of foundation*

Figures 8–10 show the observed and computed variations of uplift load and rotation angle of the foundations against the displacements of the foundation in which the reinforcements are set up at different directions from the side of the foundation. In the figures the upper part of the vertical axis from x = 0 represents load in Newton, and the lower part denotes rotation angle (θ) of the foundation. In these figures, curves without marks show the results of the foundation without reinforcements. The factors α and β of the legends are described in Figure 7. Here, α is the angle of uplift loading which is measured from the vertical direction, while β denotes the placement angle of reinforcement which is measured from the horizontal direction. It can be seen from Figure 8(a) that the reinforcements protruded diagonally downward from the side of the foundation is the most effective against vertical uplift loading. The results of the diagonally upward and the horizontal reinforcements are almost same, but smaller than that of the diagonally downward reinforcement. The observed and the computed results are similar to those obtained in the previous works (Nakai et al., 2001). The results are also very much close to the results of the two-dimensional analysis (Fig.15). The results of two-dimensional analysis (Hinokio et al, 2007) are illustrated in the APPENDIX. This research is conducted using the flexible reinforcements which act as tensile reinforcements alone.

From Figures 9 and 10, it is revealed that for the inclined uplift loading the reinforcements set up at the side of the foundation are not as effective as observed for the vertical uplift loading regardless the placement angles of the reinforcement. Although for the

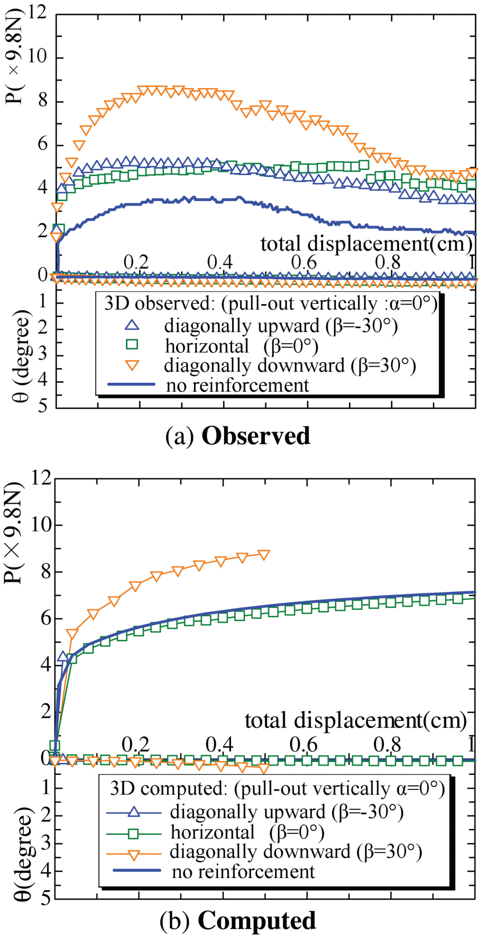

Figure 8. Load and rotation vs. displacement under vertical uplift loading ($\alpha = 0°$): reinforcements protruded from side.

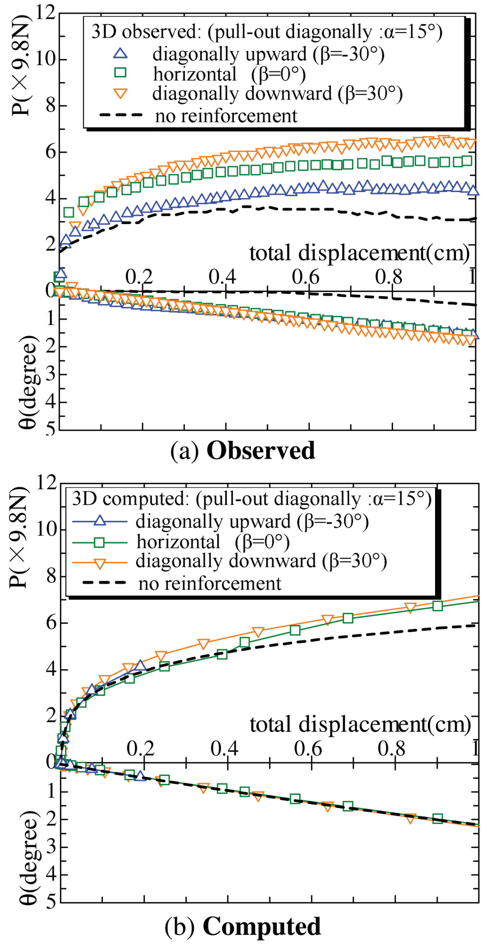

Figure 9. Load and rotation vs. displacement under inclined uplift loading ($\alpha = 15°$): reinforcements protruded from side.

3D condition the movement inside the ground is not possible to visualize by taking the photographs of the ground unlike the 2D condition, we can guess that for the diagonally downward reinforcements the deformed zone of the ground spreads wider region from the position of the reinforcements compare to the other positions of the reinforcements. For this reason, the diagonally downward reinforcements have still advantage over the horizontal and diagonally upward reinforcements. In the case of the inclined uplift loading, the frictional force between the ground and the reinforcements in the loading side works in the upward direction and acts as a negative resistance which diminishes the positive resistance of the reinforcements of the other side. Hence, the effectiveness of the reinforcements decreases with the increase of the inclination of the uplift loading. The computed results capture well the observed behavior of the foundations qualitatively and quantitatively. The observed and computed results appear to be in agreement with the results of the two-dimensional observation (Figs.16 and 17).

3.2 *Reinforcements protruded from the bottom of foundation*

Figures 12 to 14 show the observed and computed results of uplift load and rotation angle of the foundation, in which the reinforcements are protruded from the bottom of the foundation. Figure 11 denotes the description of angles α and β, where $\beta = 90°$ represents the reinforcement placed in the vertically downward direction. It is seen from these figures that these types of reinforcements increase the uplift bearing capacity significantly not only against vertical uplift load but also against inclined uplift load. Though the

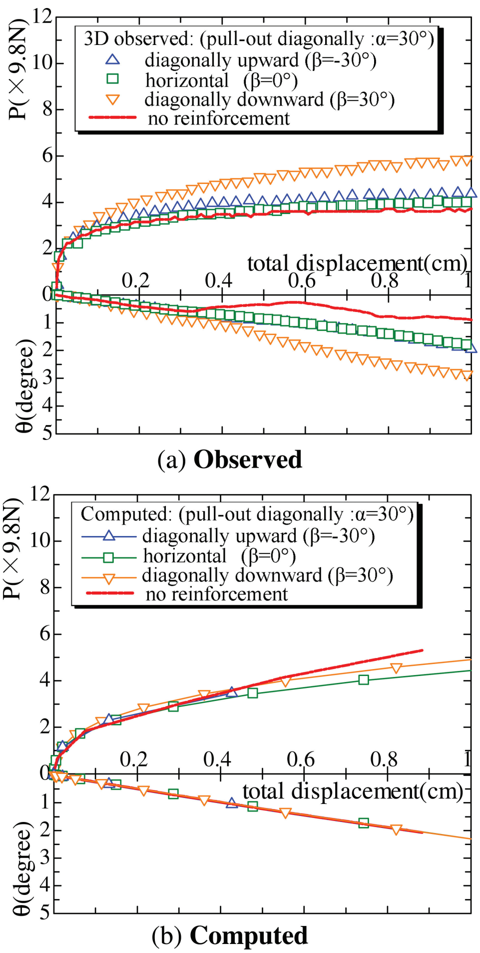

Figure 10. Load and rotation vs. displacement under inclined uplift loading ($\alpha = 30°$): reinforcements protruded from side.

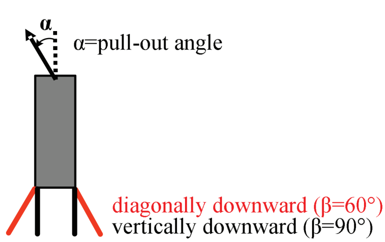

Figure 11. Description of reinforcement protruded from bottom.

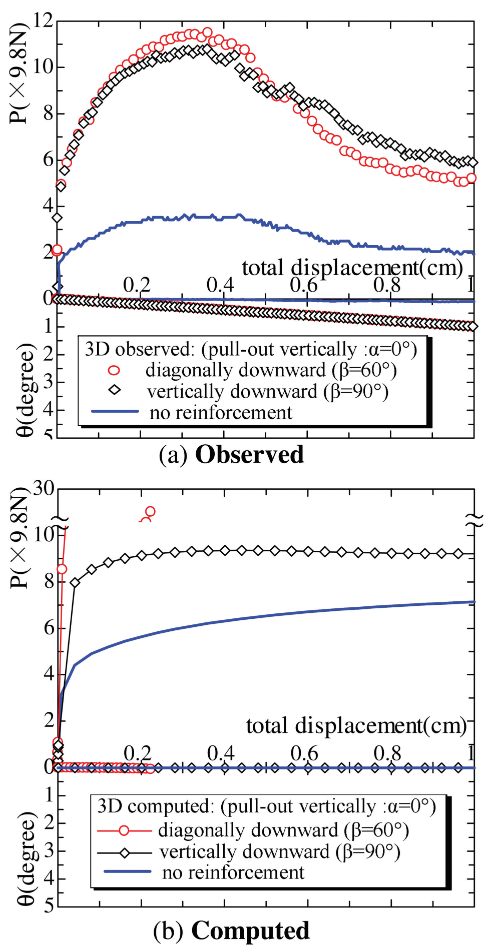

Figure 12. Load and rotation vs. displacement under vertical uplift loading ($\alpha = 0°$): reinforcements protruded from bottom.

uplift bearing capacity for diagonally downward and vertically downward reinforcements is almost same in the model tests, in the numerical analyses it is slightly larger for the diagonally downward reinforcement than that for the vertically downward reinforcement. However, there are good agreement between the results of the model tests and the numerical simulations. There are also quite similarities of the results of the three-dimensional model tests and numerical analyses with the two-dimensional ones (Figs.18 to 20). Therefore, it can be said that the 2D model tests can represent well the behavior of 3D model tests in general three-dimensional stress conditions. Similar to the model tests 2D plane strain analyses well simulate the behavior of general three-dimensional stress condition in predicting the uplift bearing capacity. Comparing the results of the reinforcements protruded from the side with the reinforcements set up at the bottom, it is found that the uplift bearing capacity for the later case is much larger than that for the former one for both loading conditions.

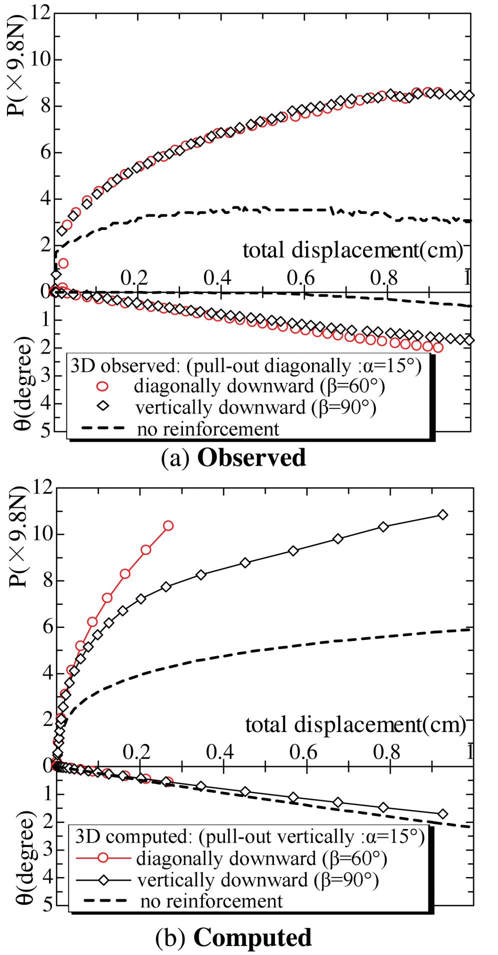

Figure 13. Load and rotation vs. displacement under inclined uplift loading ($\alpha = 15°$): reinforcements protruded from bottom.

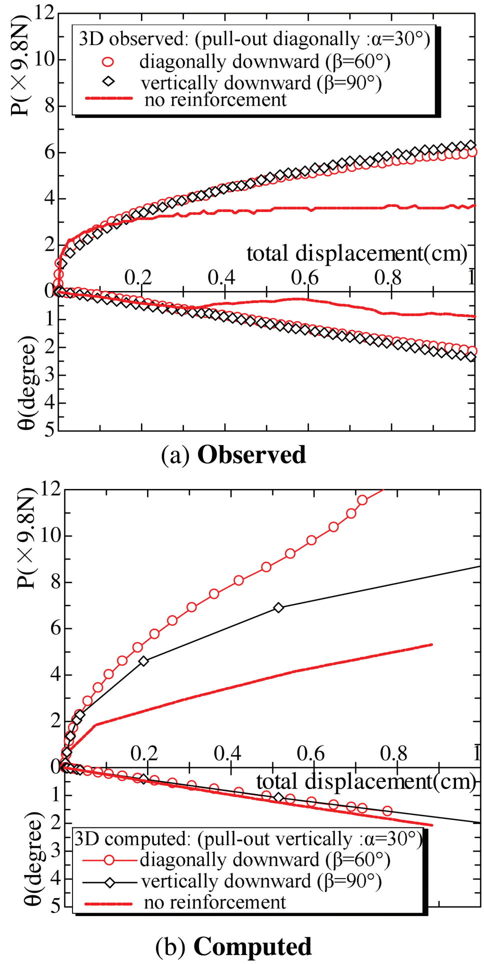

Figure 14. Load and rotation vs. displacement under inclined uplift loading ($\alpha = 30°$): reinforcements protruded from bottom.

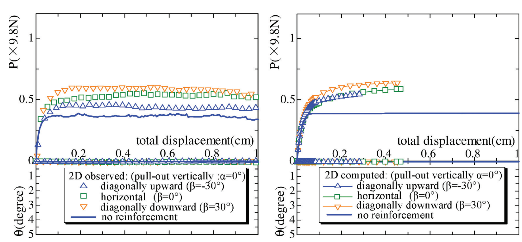

Figure 15. Load and rotation vs. displacement under vertical uplift loading ($\alpha = 0°$): reinforcements protruded from side.

4 CONCLUSIONS

The following conclusions are obtained from the model tests and numerical simulations of the reinforced foundation under uplift loadings:

(1) When reinforcement bars are set up at the side of the foundation, the reinforcements protruded diagonally downward is the most effective against vertically uplift loading. However, the reinforcement set up at the side of the foundation is not effective against inclined uplift loading (inclination angles of the uplift loads are 15° and 30° in the present study).

(2) The reinforcements which are protruded downward from the bottom of the foundation are effective not only under vertical uplift loading but also inclined uplift loading.

(3) 2D model tests and numerical analyses can represent well the behavior of 3D model tests and

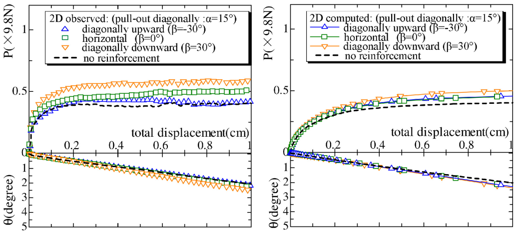

Figure 16. Load and rotation vs. displacement under inclined uplift loading ($\alpha = 15°$): reinforcements protruded from side.

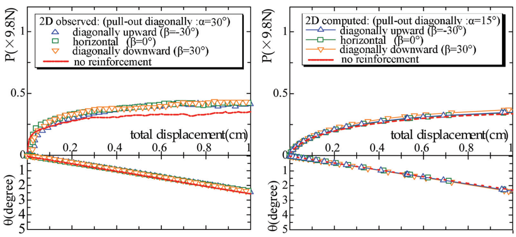

Figure 17. Load and rotation vs. displacement under inclined uplift loading ($\alpha = 30°$): reinforcements protruded from side.

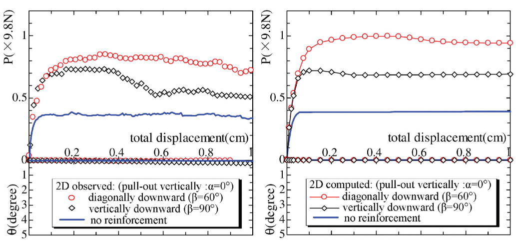

Figure 18. Load and rotation vs. displacement under vertical uplift loading ($\alpha = 0°$): reinforcements protruded from bottom.

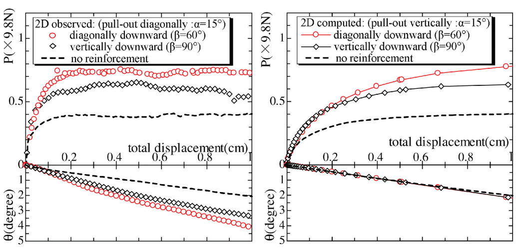

Figure 19. Load and rotation vs. displacement under inclined uplift loading ($\alpha = 15°$): reinforcements protruded from bottom.

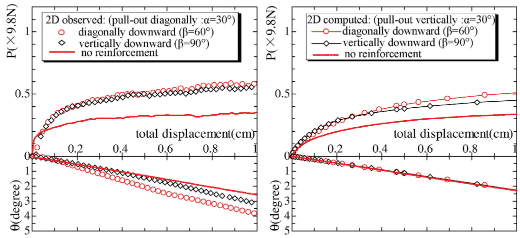

Figure 20. Load and rotation vs. displacement under inclined uplift loading ($\alpha = 30°$): reinforcements protruded from bottom.

numerical analyses in general three-dimensional stress conditions.

The analysis in which typical mechanical behavior of soils is appropriately taken into account can predict well the behavior of the reinforced foundation under uplift loading.

REFERENCES

Hinokio, M., Nakai, T., Yohona, S. and Nishio, A. (2007): Bearing capacity of reinforced foundation subjected to pull-out loading and its reinforced mechanism, Proc. of 13th Asian Regional Conference on Soil Mechanics and Geotechnical Engineering, India, December (in press).

Matsuo, M. and Ueno, M.(1989) – Development of ground reinforcing type of foundation, Proc. of 12th ICSMFE, 2, pp1205–1208.

Nakai, T. (1989) – Finite element computations for active and passive earth pressure of retaining wall, Soils and Foundatons, 25(3), 98–112.

Nakai, T., and Hinokio, M. (2004) – A simple elastoplastic model for normally and over consolidated soils with unified material parameters. Soils and Foundations. 44(2): 53–70.

Nakai, T., Teranishi, T., Hinokio, M. and Adachi, K. (2001) – Behavior of reinforced foundation under uplift and push-in loading: model tests and analyses, Proc. of IS-Kyushyu 2001, 593–598.

Tokyo Electric Power Company and Dai Nippon Construction (1990) – Report on bearing capacity of caisson type foundation with reinforcing bars, 4, (in Japanese).

APPENDIX: RESULTS OF 2D CONDITION

The results of the two-dimensional model tests and numerical analyses conducted by the authors (Hinokio et al, 2007) are illustrated in this section for the comparison with the results of the three-dimensional condition.